

Investigation of optical properties of $\text{Se}_{75}\text{Te}_{25-x}\text{Ge}_x$ ($X=0, 2, 4, 6$ and 8) thin film

¹S. M. Salem, ²H. Zayied, ^{1,3}A. M. Salem, ⁴G.B. Sakr and ¹N. Teleb

¹Electron Microscope and Thin Films Department, National Research Centre, Dokki, Giza,

²Physics Department, College of Girls for Arts, Science and Education, University of Ain Shams, Cairo, Egypt.

³University College-Umm Al-Qura University, Saudi Arabia Kingdom.

⁴Physics Department, Faculty of Education, University of Ain Shams, Cairo, Egypt.

Received: 25 Oct. 2016 / Accepted: 30 November 2016 / Publication date: 10 December 2016

ABSTRACT

Pulsed laser deposition technique was used for preparation of $\text{Se}_{75}\text{Te}_{25-x}\text{Ge}_x$ ($X=0, 2, 4, 6$ and 8) thin films. The optical parameters like "K", "N" and "α" of the deposited films were investigated using the transmission and reflection measurements. According to the WDD model, the dispersion energy " E_d ", absorption coefficient, optical dielectric constant and optical band gap were studied. The correlation between the optical band gap " E_g " and both cohesive energy and refractive index was also illustrated

Key words: Pulsed laser, thin films, transmission, reflection.

Introduction

The exceptional properties of amorphous semiconductors What's more their point of preparation utilizing thin film processes which did not restrain their size and make them suitable to integration with other solid state technologies (Pankaj and Katyal, 2008). In low characteristic phonon energies (~ 50 – 450 cm^{-1}) even relative to fluoride glasses (~ 550 cm^{-1}) Chalcogenide glasses are having relatively high atomic mass and weak bond strength, hence, these are highly transparent in the mid to far infrared. They are used in the IR windows and optics (Zhang *et al.*, 2003). The consideration in this paper is focused on chalcogenide glasses because they show many interesting properties in addition to be promising multipurpose materials in several applications. Specially, the threshold and memory switching behavior and the infrared transmission of these glasses aggravate them possibility materials for using Previously, memory devices Furthermore infrared optical fiber applications (Adler, 1997; Savage *et al.*, 1980; Kastner *et al.*, 1976; Nermec *et al.*, 2002). Also, the physical properties about chalcogenide glasses are strongly reliant on their compositions (Mott and Davis, 1979; Davis, 1973). In the display paper, an endeavor has been made to study the impact from claiming alloying "Ge" with chalcogenide "Te" atoms in $\text{Se}_{75}\text{Te}_{25-x}\text{Ge}_x$ films with ($0 \leq x \leq 8$).

Experimental

Series of $\text{Se}_{75}\text{Te}_{25-x}\text{Ge}_x$ [$x=0, 2, 4, 6, \text{and } 8$] ingot materials were prepared by direct fusion of stoichiometric proportions of pure (99.999 %) elements of "Se", "Te" and "Ge". The stoichiometric amounts of the elements were contained in the precleaned silica tube, sealed under vacuum at 10^{-3} Pa. The tubes were heated in an electrical furnace with a temperature rate of 3–4K/min up to 1050 K for 18h. During the heating process, the tubes were frequently shaken to ensure the homogeneity of the samples. The molten sample was then rapidly quenched in the ice-cooled water to obtain the desired alloys in their glassy state.

$\text{Se}_{75}\text{Te}_{25-x}\text{Ge}_x$ thin films were deposited on glass substrates using Pulsed Laser Deposition technique (PLD). with a neodymium -doped yttrium aluminum garnet (Nd:YAG) laser (Coherent US) under a laser excitation wavelength of 1064 nm. The system operating in the so-called Q-switching mode with an output powers of 250 megawatts for pulse durations of 10 to 25 nanoseconds (Robert Eason; 2007). A double beam spectrophotometer, with automatic computer data acquisition (Type Jasco, V-570, Rer11-00, and UV-VIS-NIR) was used at a normal light incidence to record the optical transmission and reflection spectra of all the deposited films in the wavelength range of 500–2500 nm. The thickness of the deposited

Corresponding Author: N. Teleb, Electron Microscope and Thin Films Department, National Research Centre, Dokki, Giza, Egypt.
E-mail: n_sleam@yahoo.com

films was determined experimentally using a Dektak 3 profilometer device and also confirmed analytically by interferometry. $\text{Se}_{75}\text{Te}_{25-x}\text{Ge}_x$ thin films were deposited at room temperature.

Results and Discussion

The transmittance, $T(\lambda)$ and reflectance, $R(\lambda)$ spectra of the ternaries $\text{Se}_{75}\text{Te}_{25-x}\text{Ge}_x$ thin film samples; curve (a) $x=0$, (b) $x=1.41$, (c) $x=3.4$, (d) $x=5.72$ and (e) $x=7.87$, where x represent the exact Ge at % resolved from the EDX measurements. It will be clear that, those transmittance spectra might be separated under three significant uncommon regions: (i) basic absorption region, which may be those district broadened in the optical wavelength extent 500-850 nm (ii) weak absorption regions, extended from $\lambda = 850$ nm to 2000 nm. What's more (iii) the transparent region, beyond $\lambda > 2000$ nm; at which sum of transmittance and reflectance was found to be almost in the order of the unity as shown in Fig 1, demonstrating that no scattering or absorption has been occurs in this region. In the weak absorption region, an interference fringe patterns were apparent, indicating that the interfaces, air/film. Furthermore film/glass were flat and parallel which reflects an optical homogeneity of the film thickness. It has been also noted that the essential absorption edge is shifted toward the higher energy (blue shift) with expanding "Ge" from 1.42 to 7.87 at % in the $\text{Se}_{75}\text{Te}_{25-x}\text{Ge}_x$ system concerning illustration demonstrate in fig 2.

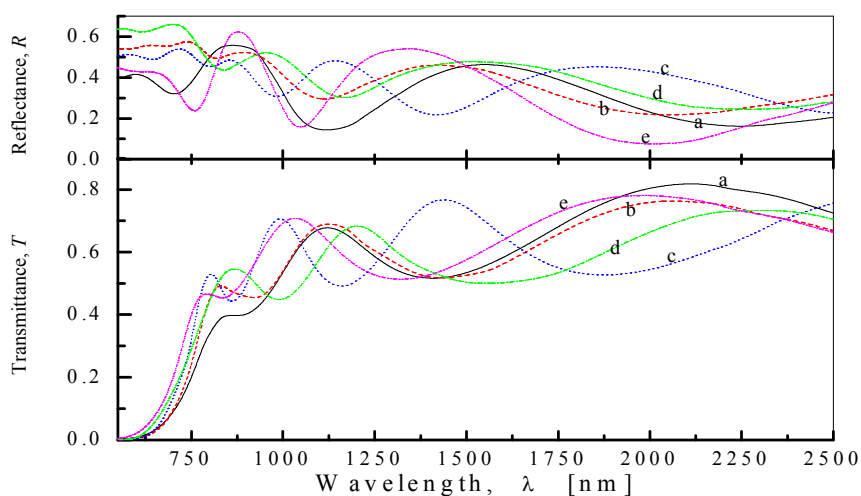


Fig. 1: Shows the transmittance and reflectance spectra of $\text{Se}_{75}\text{Te}_{25-x}\text{Ge}_x$ thin films; with exact Ge at % (a) $x=0$, (b) $x=1.41$, (c) $x=3.4$, (d) $x=5.72$ and (e) $x=7.87$, respectively.

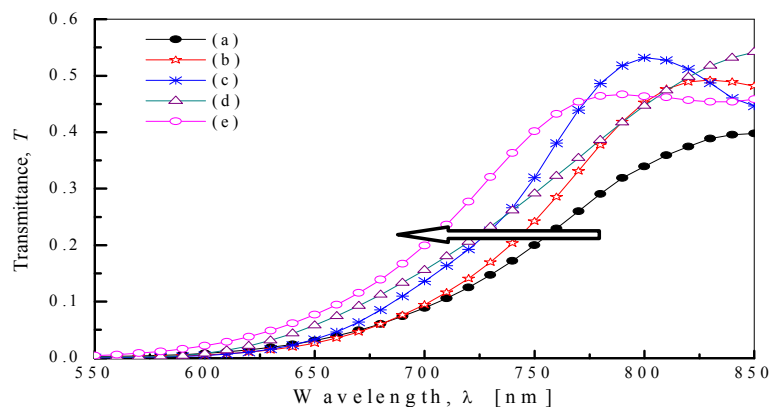


Fig. 2: Illustrates the variation of the fundamental absorption edge of $\text{Se}_{75}\text{Te}_{25-x}\text{Ge}_x$ thin films shown in figure 1 vs. wavelength.

Optical constants of $\text{Se}_{75}\text{Te}_{25-x}\text{Ge}_x$ thin films ternary system:

The thermally evaporated films have thickness " d " and complex refractive index $N = n - ik$, where n is the refractive index and " k " the extinction coefficient. Murmann's exact equations require initial values of the film refractive index, n_i furthermore extinction coefficient, " k_i ", were acquired utilizing the Swanepoel strategy (Swanepoel, 1983). As stated by Swanepoel those initial values of the refractive index and the thickness be calculated in the region at which, $\alpha \approx 0$, utilizing the relation:

$$n_i = \sqrt{N + \sqrt{N^2 - n_s^2}} \quad (1)$$

Where

$$N = 2n_s \frac{T_{\max} - T_{\min}}{T_{\max} T_{\min}} + \frac{n_s^2 + 1}{2} \quad (2)$$

Where " n_s " the refractive index of the substrate and " T_{\max} " and " T_{\min} " are the transmission maximum and the corresponding minimum at a certain wavelength. Alternatively, one of these values is an experimentally recorded (maximum or minimum) and the other one is derived from the corresponding envelope. Additionally, if " n_1 " and " n_2 " are the refractive indices at two adjacent tangent points at wavelengths " λ_1 " and " λ_2 ", using the basic equation for interference fringes (Swanepoel, 1983):

$$2nd = m\lambda \quad (3)$$

Where " m " is an order number, the thickness of the deposited film is given by:

$$d = \frac{\lambda_1 \lambda_2}{2(\lambda_1 n_2 - \lambda_2 n_1)} \quad (4)$$

Knowing the film thickness " d ", the initial values of the optical absorption coefficient, " α_i " could be determined from the measurements of $T(\lambda)$ and $R(\lambda)$ by using the well-known relation (Pankove, 1971; Qasrawi, 2007):

$$T(\lambda) = (1 - R^2)e^{-\alpha_i d} \quad (5)$$

$$\alpha_i = \frac{1}{d} \ln \frac{(1-R^2)}{T} \quad (6)$$

Sequent, the initial values of the extinction coefficient, " k_i " can be calculated using the relation:

$$k_i = \frac{\alpha_i \lambda}{4\pi} \quad (7)$$

Therefore, using the experimental values of the transmittance and reflectance and the initial values of the film refractive index, " n_i " and extinction coefficient, " k_i ", the accurate values of the film refractive index, " n " and extinction coefficient, " k " were computed using the following computer program based on minimizing the values of $(\Delta T)^2 = (T_{n_i k_i} - T_{\text{exp}})^2$ and $(\Delta R)^2 = (R_{n_i k_i} - R_{\text{exp}})^2$ simultaneously and solving Murmann's exact equations.

The spectral variation of the extinction coefficient, " k " (in the fundamental absorption region 550-850 nm) and the refractive index, " n " (over the whole spectral range 550-2500 nm) for the investigated samples with different "Ge" content, applying the computational program based on Murmann's equations are shown in Fig.3.

The refractive indices curves of the investigated samples as a function of wavelength have been aggregated together concerning illustration demonstrated over fig. 4. It has been realized that the behavior of the refractive index, n has higher value at the strong absorption region (550-850 nm), display anomalous dispersion behavior, The anomalous dispersion behavior of the refractive index could be attributed to the resonance effect between the incident electromagnetic radiation and the electron polarization (El-Nahass *et al.*, 2012; Hassanien and Akl, 2015). In the anomalous dispersion region the refractive index n attains peak observed in the wavelength range 640-780 nm. Beyond the strong absorption region 850-2500 nm the refractive index sharply decreases with increasing wavelength, the magnitude of the refractive index at certain wavelength value in the anomalous dispersion region decreases with expanding Ge in the ternary $\text{Se}_{75}\text{Te}_{25-x}\text{Ge}_x$ system from 1.41 to 7.87 at %.

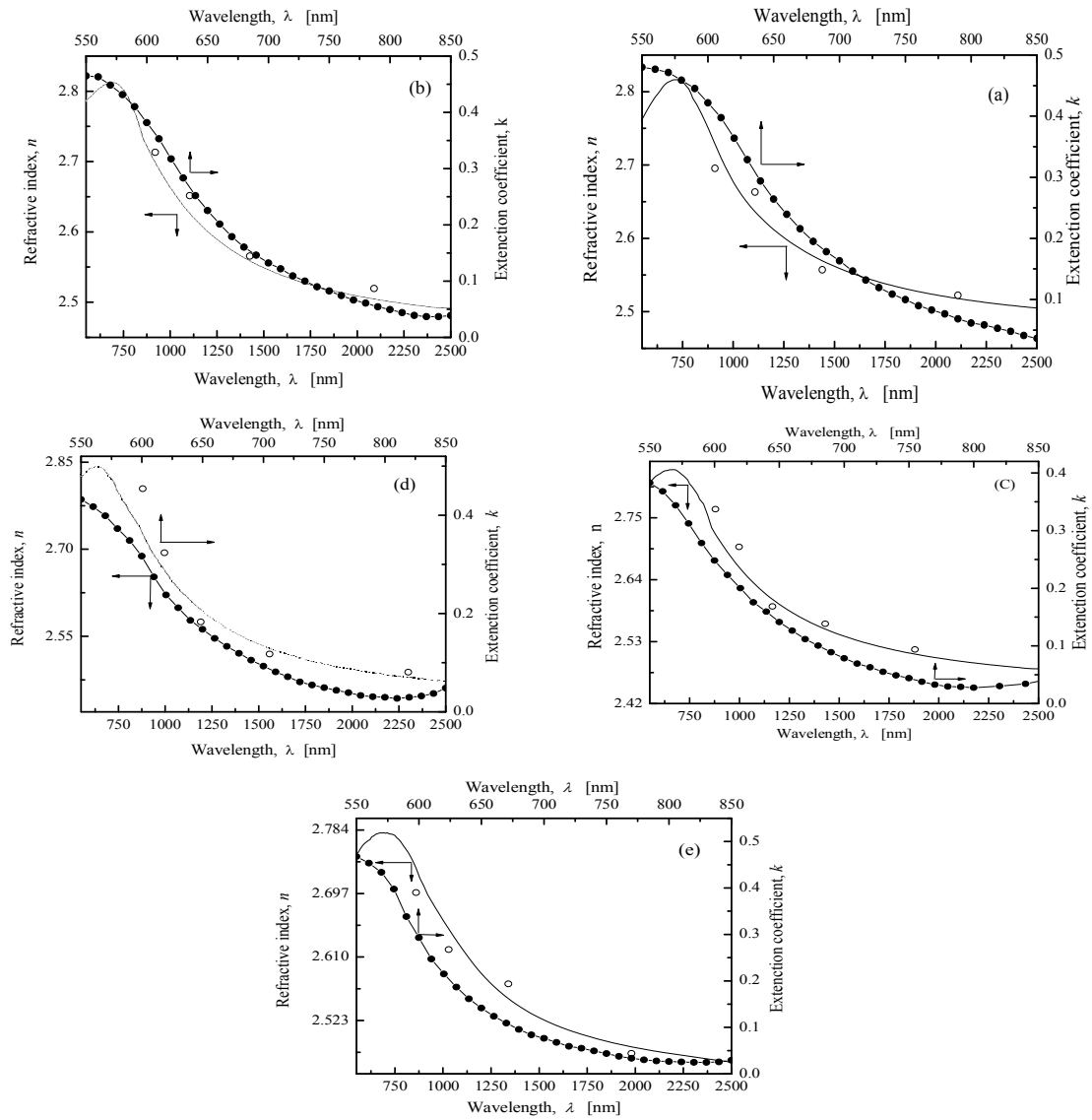


Fig. 3: shows the spectral variation of the refractive index, n and extinction coefficient, k as a function of wavelength. The circle open symbol represents the initial values of the refractive index calculated using Swanepoel method.

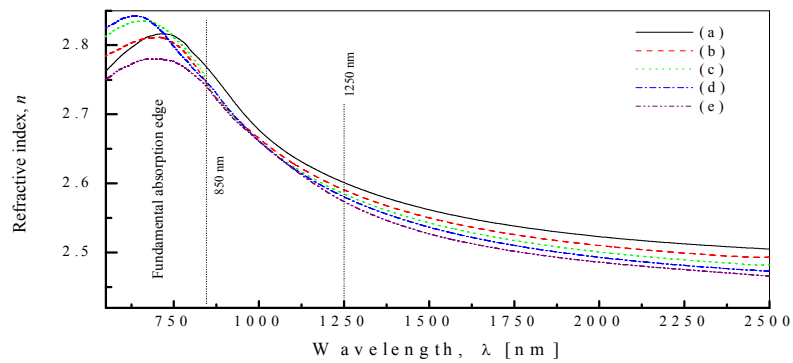


Fig. 4: variation of the refractive index as a function of wavelength, for samples a-e.

Determination of the dielectric constants for the ternary $\text{Se}_{75}\text{Te}_{25-x}\text{Ge}_x$ thin films:

The gotten refractive index information might make further investigated to acquire the high frequency dielectric constant by means of two methods. The initial technique depicts the contribution of the free carriers and the lattice vibration modes of the dispersion, from which one can acquire the lattice dielectric constant (Spitzer and Fan, 1957). The second procedure is based upon the dispersion arising from the bound carriers over an empty lattice (Moss, 1959). Two methods been utilizing for acquiring a reliable value for the high frequency dielectric constant.

First procedure:

According to Spitzer and Fan model, (1957); the relation between the lattice dielectric constant, " ϵ_L ", and the refractive index, " n ", is given by the relation.

$$\epsilon_r = \epsilon_L - A\lambda^2 \tag{8}$$

Where

$$A = \frac{e^2 N}{4\pi^2 c^2 \epsilon_0 m^*}$$

Where " ϵ_r " is the real part of dielectric constant, " ϵ_L " is the lattice dielectric constant or (the high frequency dielectric constant). According to first procedure, " λ " is the wavelength, " N " is the free charge carrier concentration, " ϵ_0 " is the permittivity of free space (8.854×10^{-12} F/m), m^* is the effective mass of the charge carrier and " c " is the velocity of light. The real part of the dielectric constant $\epsilon_r = n^2 - k^2$ was calculated at different values of " λ " in the transparent region. Then, the obtained values of " ϵ_r " are plotted as a function of " λ^2 " as shown in Figure5

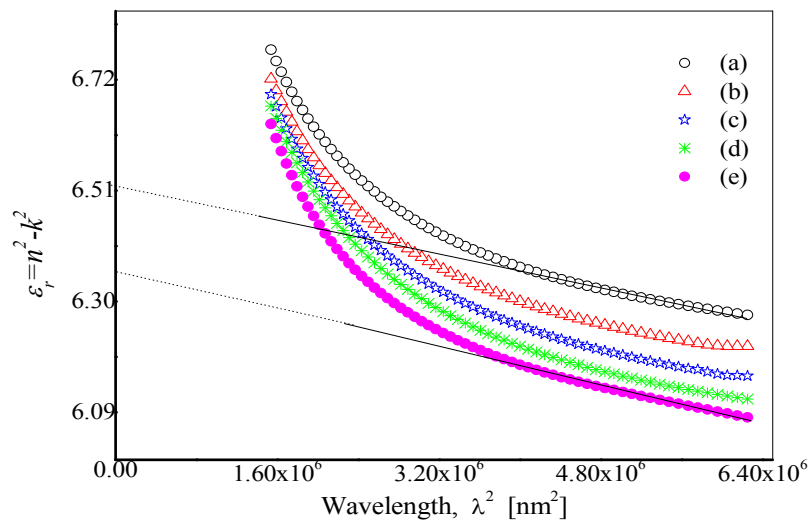


Fig. 5: Plots of ϵ_r vs. λ^2 the ternary $\text{Se}_{75}\text{Te}_{25-x}\text{Ge}_x$ system.

Furthermore, in the transparency range, when $n^2 \ll k^2$ and $\ll 1$; where " ω " is the angular frequency ($\omega = 2\pi c/\lambda$) and " τ " is the relaxation time, the real part of the dielectric constant " ϵ_r " can be written as (Osama *et al.*, 2009; Koteeswara and Reddy, 2006).

$$\epsilon_r = \epsilon_L - \frac{\omega_p^2}{\omega^2} \tag{9}$$

$$\omega_p^2 = \frac{e^2 \cdot N / m^*}{\epsilon_0}$$

Where " ω_p " is the plasma frequency, the calculated values of " ϵ_L ", N/m^* as well as the plasma frequency, " ω_p " for the ternary $\text{Se}_{75}\text{Te}_{25-x}\text{Ge}_x$ system are given in Table 1. It has been observed that the

calculated values of " ϵ_L ", N/m^* and the plasma frequency " ω_p " are decreases with the increase of "Ge" content at % (in the studied

Table 1: value of ϵ_L , N/m^* as well as the plasma frequency ω_p for the ternary $Se_{75}Te_{25-x}Ge_x$ system.

Ge at %	ϵ_L	$N/m^* (\times 10^{55})$ ($Kg.m^3$) ⁻¹	$\omega_p (\times 10^{14})$ (Hz)	ϵ_∞	λ_o (nm)	$S_o(\times 10^{13})$ (m^{-2})
0	6.59	0.87	4.63	6.13	416.7	1.12
1.41	6.54	0.82	4.57	6.06	423.5	1.10
3.40	6.51	0.77	4.49	6.01	433.9	1.06
5.72	6.45	0.75	4.44	5.96	442.1	1.03
7.87	6.42	0.72	4.25	5.93	436.9	1.02

The second procedures:

The dielectric constant of the material could be calculated using the dispersion relation of the incident photon. The refractive index was also fitted using a function for extrapolation towards the shorter wavelengths. The model of Moss (Koteeswara and Reddy, 2006) which stated that, the free carrier contribution to dispersion is relatively small. This means that data corresponding to the wavelength range lying below the absorption edge of the material are to be used. The properties of the investigated sample could be treated as a single-oscillator at wavelength " λ_o " at the higher frequency. The high frequency dielectric constant can be calculated by applying the following simple classical dispersion relation (Koteeswara and Reddy, 2006; Wahab *et al.*, 2012).

$$(n^2 - 1)^{-1} = (n_o^2 - 1)^{-1} - \lambda_o^2 = (n_o^2 - 1)^{-1} \lambda^{-2} \quad (10)$$

Where " n_o " is the refractive index at infinite wavelength " λ_o " (average interband oscillator wavelength), " n " is the refractive index and " λ " is the wavelength of the incident photon where:

$$(n^2 - 1) = \left(\frac{S_o \lambda_o^2}{1 - (\lambda^2 / \lambda_o^2)} \right) \quad (11)$$

Where, " S_o " is the average oscillator strength given by;

$$S_o = \frac{n_o^2 - 1}{\lambda_o^2}$$

Therefore, plotting $(n^2 - 1)^{-1}$ vs. λ^{-2} in the wavelength range 1250-2500 nm, as shown in Fig. 6 exhibits a linear part at the transparent region. The values of " S_o ", " λ_o " and " ϵ_∞ " for the investigated compositions can be determined from the linear fit of this plot. These values are listed in Table 1. From this table, it has been observed that, the values of " S_o " and " ϵ_∞ " are decreased with increase "Ge" content, while the values of " λ_o " are increased. It has been also observed from the data summarized in Table 1 that, the values of the static dielectric constant obtained according to the WDD model, agree very well with the corresponding values obtained in the second procedure based on the Moss model, however, these values are slightly lower than the values of the lattice dielectric constant obtained according to Spitzer and Fan model (Parlak *et al.*; 2003; El-Nahass *et al.*, 2004; Qasrawi and Ahmad, 2006). This disagreement between the values of the lattice dielectric constant and static dielectric constant can be attributed to contribution of the free carriers to the effective mass ratio in the Spitzer and Fan model. Similar conclusion has been reported for the other binary and ternary chalcogenide systems (Qasrawi and Ahmad, 2006; Ammar *et al.*, 2015; Atyia and Hegab, 2014).

Absorption coefficient, and optical band gap of $Se_{75}Te_{25-x}Ge_x$ ternary system:

Optical absorption measurements estimations would use to acquire the band structure and the energy gap of binary and ternary chalcogenide thin films. Since the dissection of the optical absorption spectra may be a standout amongst those A large portion profitable tools for understanding and developing the energy band diagram of both crystalline and amorphous materials (Guoxiang *et al.*, 2012). Utilizing those computed values of " k ", the optical absorption coefficient, " α " has been calculated in the fundamental absorption region utilizing the Eq7 Fig. 7 shows the semi-logarithmic plots of (α) with photon energy for the investigated films in the region fundamental absorption region (550-850 nm). It has been observed that, for all of the investigated samples the absorption coefficient increases exponentially with the increase of photon energy and has values greater than 10^4 cm⁻¹ in the photon energy range 1.3–1.45 eV.

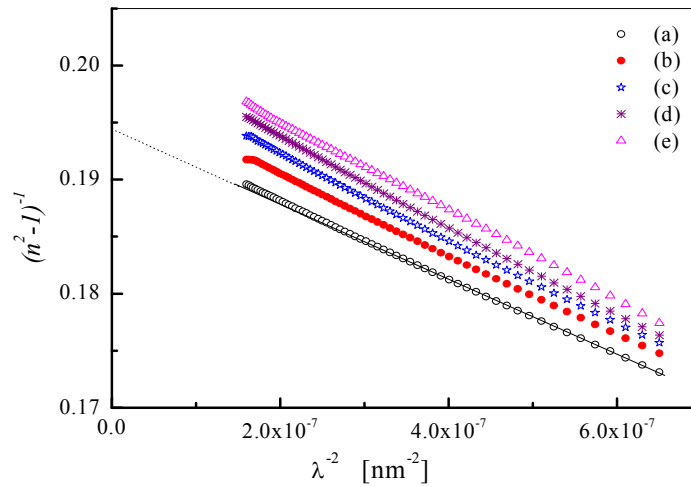


Fig. 6: plots of $(n^2 - 1)^{-1}$ vs. λ^{-2} for the ternary $\text{Se}_{75}\text{Te}_{25-x}\text{Ge}_x$ system.

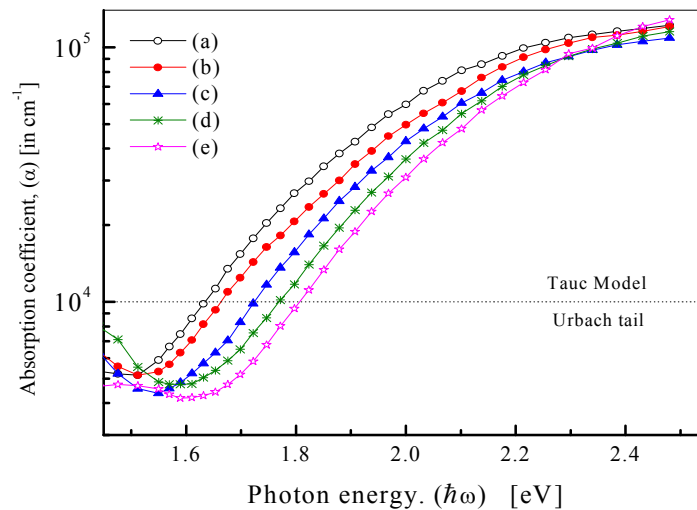


Fig. 7: spectral variation of the absorption coefficient with photon energy, for the $\text{Se}_{75}\text{Te}_{25-x}\text{Ge}_x$ ternary system.

The observed spectral can be isolated into two distinct regions:

i. High absorption region where $\alpha \geq 10^4 \text{ cm}^{-1}$. The absorption coefficient in this region is given by (Tauc, 1974; Tauc and Menth, 1972) :

$$\alpha = C(E - E_g)^{\frac{p}{\hbar\omega}} \tag{12}$$

Where C is constant relying upon the transition probability, " E_g " is the band gap also is an index that characterizes the sort of the optical absorption transition and is theoretically equal to 1/2, 2 for direct allowed and indirect allowed optical transitions, plotting an chart from $(\alpha\hbar\omega)^{1/p}$ vs. photon energy, $(\hbar\omega)$ in accordance to Eq.12 the value of " E_g ". The examination of the absorption coefficient in the working photon energy range reveals the dependence of " α " on the photon energy $(\hbar\omega)$ could be described by the relation in Eq.12 with

$p=2$, which reveals an allowed indirect optical transition involved for the investigated $\text{Se}_{75}\text{Te}_{25-x}\text{Ge}_x$ thin films ternary system (see Fig.8). The energy corresponding to this transition can be obtained as the intercept of the curve of $(\alpha\hbar\omega)^{1/2}$ vs. $(\hbar\omega)$. The determined indirect optical band gap values as a function of Ge content are listed in Table 2.

Table 2: The values of the optical band gap and energy of Urbach tail for $\text{Se}_{75}\text{Te}_{25-x}\text{Ge}_x$ thin Fig.8 films ternary system.

Ge content (at %)	E_g (eV)	E_e (meV)	E_o/E_g
0	1.31	231	2.27
1.41	1.35	196	2.16
3.40	1.38	178	2.08
5.72	1.40	173	2.04
7.87	1.43	168	1.98

- i. In the absorption region where $\alpha < 10^4 \text{cm}^{-1}$; Usually called Urbach's exponential tail region at which the absorption depends exponentially on the photon energy is given by Urbach,(1953); Fadel *et al.*, (2009):

$$(\alpha) = \alpha_o \exp(\hbar\omega/E_e) \quad (13)$$

Where α_o is a constant and E_e is interoperated as band tail width of the localized states, which generally represents the degree of the disorder in the amorphous materials. Fig.9 indicates the plots of $\ln(\alpha)$ vs. $(\hbar\omega)$; the slope of the plots $(1/E_e)$ is used to calculate the energy value of the Urbach tail, which corresponding the optical transitions take place between localized tail states Also developed band states. Those values of (E_e) are also listed in Table 2. the value of the E_g reported in table 2 were found to increments for expanding Ge content at % at the expense of Te content, same time the energy of the Urbach tail decreases. Comparative ternd to the rise of the band gap energy with adding Ge has been realized for $\text{Se}_{75}\text{Te}_{25-x}\text{Ge}_x$ system, the authors reported that while the energy of optical gap raise with increment Ge the energy of the Urbach tail decline (Urbach, 1953).The deduced indirect optical band gap energies for the display investigated framework were discovered in the scales for those WDD oscillator energy, (E_o) through the emperical relation $E_o/E_g \approx 2$ (Wemple and DiDomenico, 1971). on fact, the value of oscillator energy (E_o) (calculated from refractive index dispersion analysis beyond the fundamental absorption edge) provide quantitative information on the overall band structure of the investigated material. This worth is truly not quite the value of the optical band gap, (E_g) , which probes the optical properties of the material close the fundamental absorption edge.

Optical dielectric constant for the ternary $\text{Se}_{75}\text{Te}_{25-x}\text{Ge}_x$ system films and other related functions:

The real Furthermore imaginary parts of the dielectric constant of as-deposited ternary $\text{Se}_{75}\text{Te}_{25-x}\text{Ge}_x$ films have a chance to be ascertained with assistance of refractive index n and extinction coefficient k . By means of those well-known Eq:

$$\mathcal{E}_r = n^2 - k^2, \mathcal{E}_i = 2nk \quad (14)$$

The varity about both " \mathcal{E}_r " What's more " \mathcal{E}_i " as a function of wavelength for the films under consideration indicated in Fig. 10. It has been observed that for such of the investigated film composition, the real Furthermore imaginary parts of the dielectric constant declines intensfly with expanding wavelength in range 550-850 nm, same time, the imaginary part of the dielectric constant reach a minimum magnitude at the end of this range, while the real dielectric constant declines slowly after that. This behaviour can be understood du to the fact that the real part of the dielectric constant is associated with the term that how much it will slow down the speed of light in the material, while the imaginary part gives that how a dielectric absorb energy from electric field due to dipole motion.

Sequentially, energetic electron beams are known to loss energy when passing through a thin film in electron energy-loss spectroscopy, with the amount of the energy loss related to the free-electron density in the material. The volume - $\text{Im}(1/\mathcal{E})$ and surface - $\text{Im} 1/(\mathcal{E} + 1)$ energy-loss functions are related to the material

optical properties *via* the real, " \mathcal{E}_r "and imaginary, " \mathcal{E}_i "parts of the dielectric functions as (Abdullah, 2013; Park, 2012; Badran *et al.*, 2012):

$$-\text{Im} \left[\frac{1}{\mathcal{E}} \right] = \frac{\mathcal{E}_r}{\mathcal{E}_i^2 + \mathcal{E}_r^2} \quad (15)$$

$$-\text{Im}\left[\frac{1}{(\varepsilon + 1)}\right] = \frac{\varepsilon_r}{[(\varepsilon_i + 1)^2 + \varepsilon_r^2]}$$

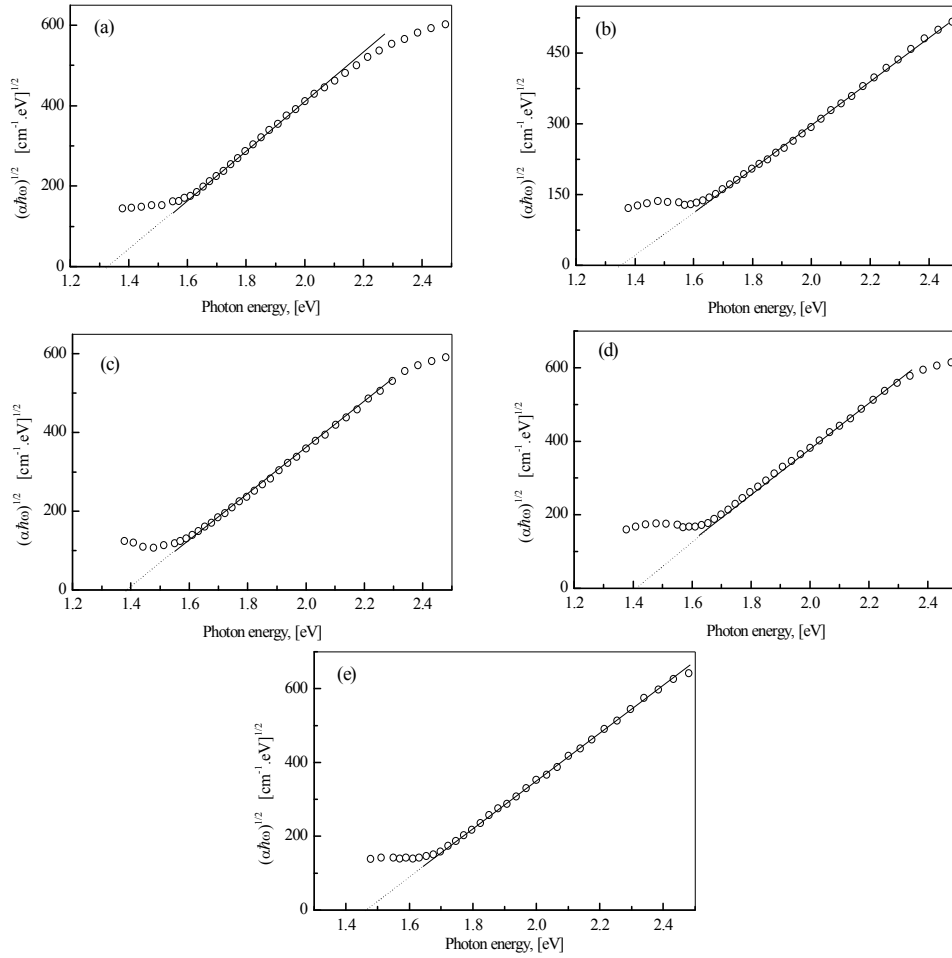


Fig. 8: Plot of $(\alpha\hbar\omega)^{1/2}$ vs. $\hbar\omega$ for $\text{Se}_{75}\text{Te}_{25-x}\text{Ge}_x$ thin films ternary system.

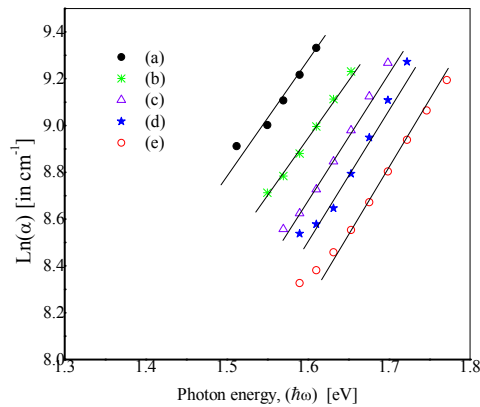


Fig. 9: Plot of $\ln(\alpha)$ vs. $\hbar\omega$ for $\text{Se}_{75}\text{Te}_{25-x}\text{Ge}_x$ thin films ternary system.

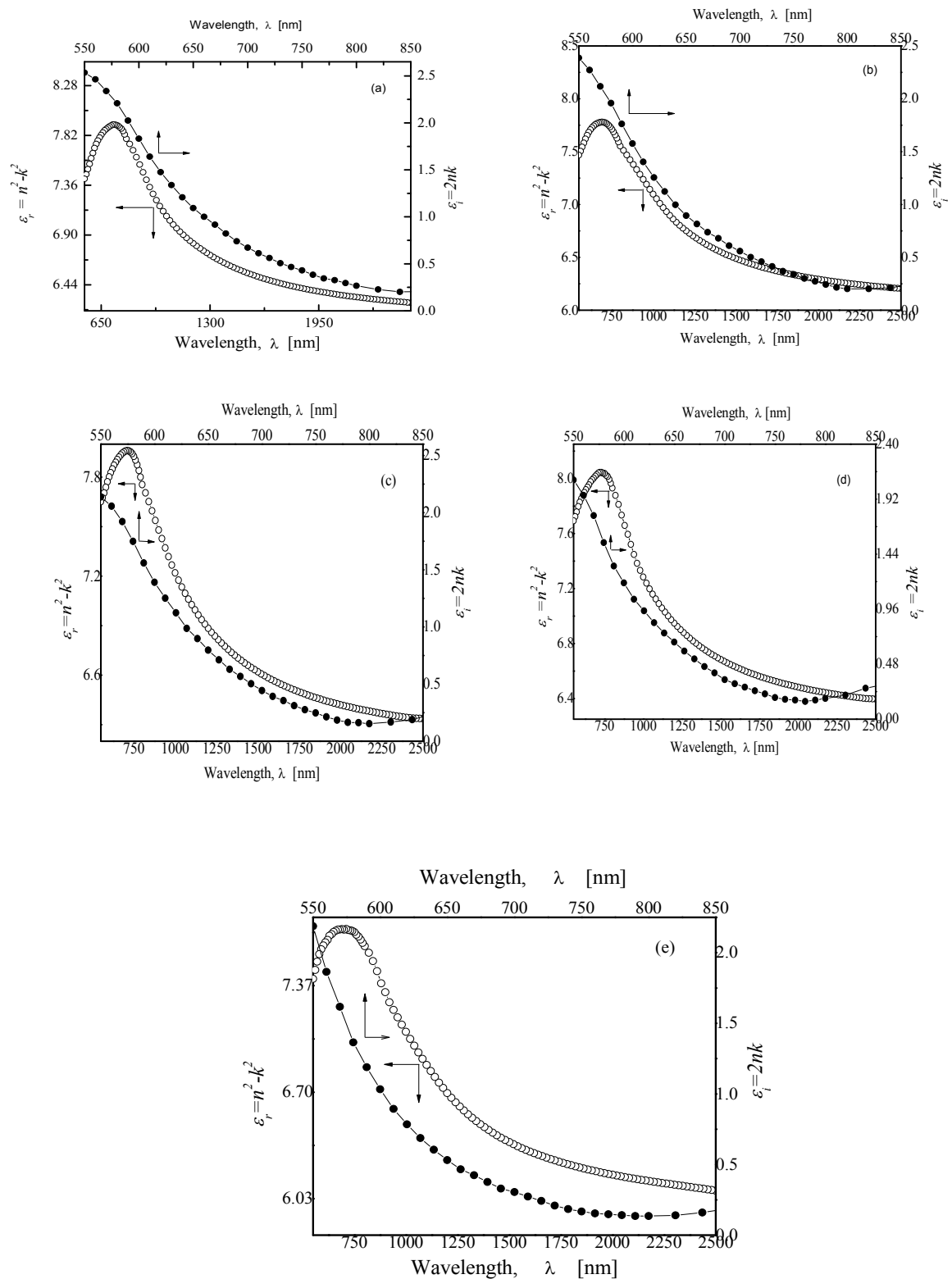


Fig. 10: spectra variation of the real and imaginary parts of the dielectric constants of the ternary system.

Figure 11 shows the graphical representation of the spectral variation of the surface and volume energy loss functions as a function of the wavelength for different values of "Ge" content. It has been observed that

for all the investigated and at any of certain value of the wavelength the magnitude of the surface energy loss is higher than the volume energy value loss.

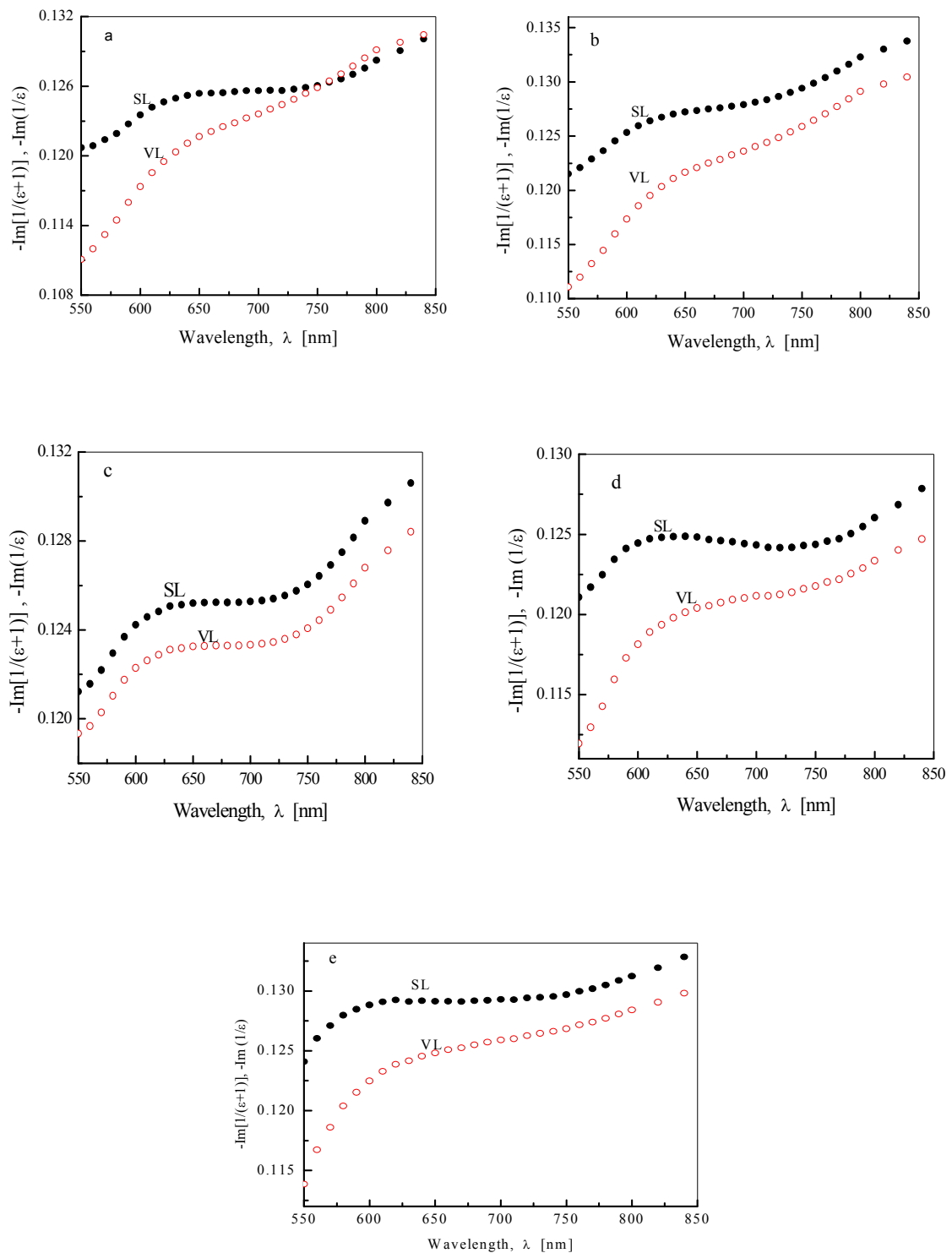


Fig. 11: Graphical representation of the surface and volume energy loss functions

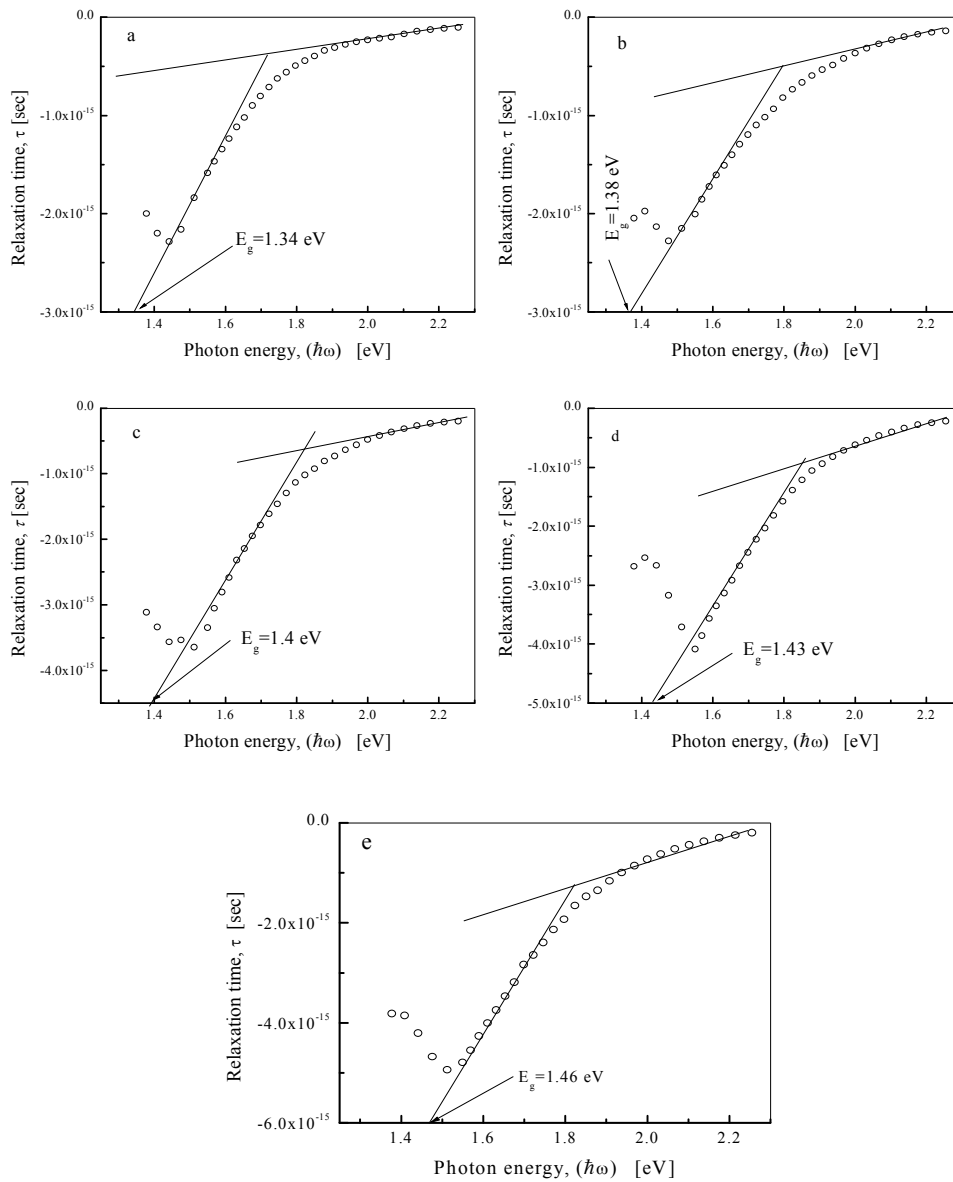


Fig. 12: Variation of the dielectric relaxation time τ as a function of photon energy, $(\hbar\omega)$ for the ternary $\text{Se}_{75}\text{Te}_{25-x}\text{Ge}_x$ thin films system.

The dielectric relaxation time, " τ " can be determined by the following equation (Bell *et al.*, 1985; Han *et al.*, 1889; El-Nahass *et al.*, 2004):

$$\tau = \frac{\epsilon_{\infty} - \epsilon_r}{\omega \epsilon_i} \quad (16)$$

where " ϵ_{∞} " is the high frequency dielectric constant (mean values of the calculated static and lattice dielectric constants). Figure 12 depicts the variation of the dielectric relaxation time " τ " as a function of photon energy, " $\hbar\omega$ " for the ternary $\text{Se}_{75}\text{Te}_{25-x}\text{Ge}_x$ thin films system.

It has been observed from Figure 12 showed that the relaxation time increase with increasing the photon energy, reach to saturation at the end of the absorption region. The value of the optical band gap " E_g " can be also estimated from this plot by extrapolation the straight line from the saturation of relaxation time at the higher photon energy to the x-axis (Sakr *et al.*, 2010).

Correlation between the optical band gap, E_g and refractive index, n

According to Penn's theory, which is applicable for chalcogenide semiconductors we have (Abdel-Aziz *et al.*, 2001)

$$n^2 = 1 + \left(\frac{\hbar\omega_p}{E_g}\right)^2 \dots \dots \dots (17)$$

where ω_p is the plasma frequency given as we are mentioned previously by the ratio:

$$\omega_p^2 = 4\pi e^2 \cdot \frac{N}{m^*}$$

where N is the free charge-carrier concentration and m^* is the effective mass of the carrier. It can be seen that, there are two competing values affects the behaviour of n^2 , namely the value of N/m^* represented in numerator and the value of E_g^2 in the denominator. Therefore, according to Eq. 17 as the E_g value increases the ratio $(N/m^*)/E_g^2$ decreases and consequently n^2 decrease. Fig.13 shows the variation of the determined optical band gap and refractive index, n^2 as well as variation of the ratio $(N/m^*)/E_g^2$ as a function of the Ge content at%.

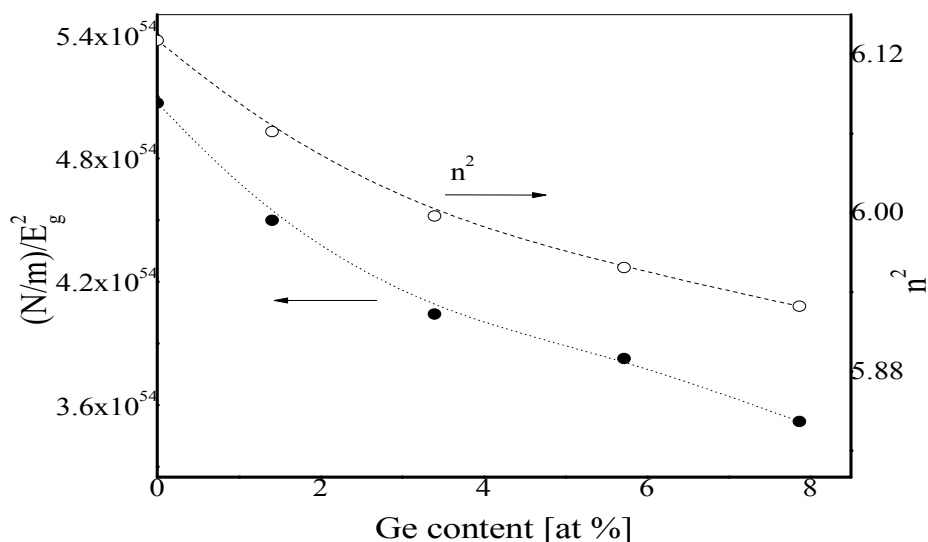


Fig. 13 : Variation of $(N/m^*)/E_g^2$ and n^2 vs. Ge content at %.

Conclusion

Studying the optical properties of $Se_{75}Te_{25-x}Ge_x$ is very interesting for qualifying of many optical constants by analyzing of the transmission and the reflection of the deposited films. The fundamental absorption edge is shifted toward the higher energy (blue shift) with increment of "Ge" from 1.42 to 7.87 at %, values of " ϵ_L ", " N/m^* " and " ω_p " are decreasing with the increasing of "Ge" at %. For all of the studied samples the absorption coefficient expanding exponentially with the increasing of photon energy also it has values greater than 10^4 cm^{-1} in the photon energy range 1.3–1.45 eV. The real also imaginary parts of the dielectric constant decreases intensely with increasing wavelength in range 550-850 nm when the real part of the dielectric constant still decreases slowly with high wavelength, the relaxation time increases with increasing the photon energy, reach to saturation at the end of the absorption region.

References

- Abdel-Aziz, M.M., E.G. El-Metwally, M. Fadel, H. H. Labib and M. A. Afifi, 2001. Optical properties of amorphous Ge-Se-Tl system films. *Thin Solid Films*, Vol.386, No.1, (May 2001), pp.99-104, ISSN 0040-6090.
- Abdullah, A., 2013. Surface and Volume Energy Loss, Optical Conductivity of Rhodamine 6G dye (R6G). *Chemistry and Materials Research*, 3 10: 56.
- Adler, D., 1977. Electronic properties of chalcogenide glasses and their use in xerography. *Sci. Am.* 36: 236.
- Ammar, A.H., A.M. Farid, A.A.M. Farag, K.A.A. Sharshar, F.S.H. Abu-Samah and K.M. Hamad, 2015. structural, absorption, dispersion and photo-induced characteristics of thermally vacuum-evaporated BiSbSe₃ thin films. *Journal of Non-Crystalline Solids*, 416: 50.
- Atyia, H.E. and N.A. Hegab, 2014. Determination and analysis of optical constants for Ge₁₅Se₆₀Bi₂₅ thin films; *Physica B* 454: 189.
- Badran, H.A., M.F. Al-Mudhaffer, Q.M.A. Hassan and A.Y. Al-Ahmad, 2012. Study of the linear optical properties and surface energyloss of 5',5"-dibromo-o-cresolsulphophthalein thin films. *Chalcogenide Letters*, 9: 483.
- Bell, R.J., M.A. Ordal and R.W. Alexander, 1985. Equations linking different sets of optical properties for nonmagnetic materials. *Appl. Opt.*, 24: 3680.
- Davis, E.A., 1973. *Electronic and Structural Properties of Amorphous Semiconductors*, Academic Press, London, New York, p: 425.
- El-Nahass, M.M., A.A.M. Farag, E.M. Ibrahim and S. Abd-El-Rahma, 2004. Structural, optical and electrical properties of thermally evaporated Ag₂S thin films. *Vacuum*, 72: 453.
- El-Nahass, M.M., I.T. Zedan and F.S. Abu-Samah, 2012. Effect of annealing on structure and optical properties of Ga₅Se₉₅ films, *Optics & Laser Technology*, 44: 621.
- Fadel, M., S.A. Fayek, M.O. Abou-Helal, M.M. Ibrahim and A.M. Shakra, 2009. Structural and optical properties of SeGe and SeGe_x (X = In, Sb and Bi) amorphous films. *Journal of Alloys and Compounds*, 485: 604.
- Guoxiang, W., Q. Nie, X. Shen, F. Chen, J. Li, W. Zhang, T. Xu and S. Dai, 2012. Phase change and optical band gap behavior of Ge-Te-Ga thin films prepared by thermal evaporation. *Vacuum* 86: 1572.
- Han, M. Y., W. Huang, C. H. Chew, and L. M. Gan, X. J. Zhang and W. Ji, 1998. Large Nonlinear Absorption in Coated Ag₂S/CdS Nanoparticles by Inverse Microemulsion. *J. Phys. Chem. B* 102: 1884.
- Hassanien, A.S. and A. A. Akl, 2015. Influence of composition on optical and dispersion parameters of thermally evaporated non-crystalline Cd₅₀S_{50-x}Se_x thin films. *Journal of Alloys and Compounds*, 648: 280.
- Kastner, M., D. Adler and H. Fritzsches, 1976. Valence-Alternation Model for Localized Gap States in Lone-Pair Semiconductors. *Phys. Rev. Lett.*, 37: 1504.
- Koteeswara, N. R. and K.T.R. Reddy, 2006. Optical behaviour of sprayed tin sulphide thin films. *Materials Research Bulletin*, 41: 414.
- Moss, T.S., 1959. *Optical Properties of Semiconductors*, Butter Worth Scientific Publication Ltd., London.
- Mott, N.F. and E.A. Davis, 1979. *Electronic Processes in Non-Crystalline Materials*, Clarendon, Oxford, p: 428.
- Nermec, P., M. Frumar, B. Frumarova, M. Jelinek, J. Lancok and I. Gregora, 2002. Thin amorphous chalcogenide films prepared by pulsed laser deposition. *J. Non-Cryst. Solids*, 299-302.
- Osama, A., Azim, M.M. Abdel-Aziz and I.S. Yahia, 2009. Structure and optical analysis of Ta₂O₅ deposited on infrasil substrate, *Applied Surface Science*, 255: 4829.
- Pankaj, S. and S.C. Katyal, 2008. Far-infrared transmission and bonding arrangement in Ge₁₀Se_{90-x}Te_x semiconducting glassy alloys, 354: 3836-3839.
- Pankove, J.I., 1971. *Optical Processes in Semiconductors*, Prentice- Hall, New Jersey, p: 93.
- Park, W.D., 2012. Optical Constants and Dispersion Parameters of CdS Thin Film Prepared by Chemical Bath Deposition. *Trans. Electr. Electron. Mater.*, 13: 196.
- Parlak, M., A.F. Qasrawi and C. Ercelebi, 2003. Growth, electrical and structural characterization of β-GaSe thin films. *J.Mater. Sci.*, 38: 1507.

- Qasrawi, A.F., 2007. Temperature dependence of the band gap, refractive index and single-oscillator parameters of amorphous indium selenide thin films. *Optical Materials*, 29: 1751.
- Qasrawi, F.A and M. M. S. Ahmad, 2006. Optoelectrical properties of polycrystalline β -GaSe thin films. *Cryst. Res. Technol.*, 41: 364.
- Sakr, G.B., I.S. Yahia, M. Fadel, S.S. Fouad and N. Romcevi, 2010. Optical spectroscopy, optical conductivity, dielectric properties and new methods for determining the gap states of CuSe thin films. *Journal of Alloys and Compounds*, 507: 557.
- Savage, J.A., P.J. Webber and A.M. Pitt, 1980. The potential of Ge-As-Te glasses as 3-5 μ m and 8-12 μ m infrared optical materials. *Infrared Phys*, 20: 313.
- Spitzer, W.G. and H.Y. Fan, 1957. Determination of Optical Constants and Carrier Effective Mass of Semiconductors. *Phys. Rev.*, 106: 882.
- Swanepoel, R., 1983. Determination of the thickness and optical constants of amorphous silicon. *Journal of Physics E* 16: 1214.
- Tauc, J and A. Menth, 1972. States in the gap. *J. Non-Crystal Solids*, 8: 569.
- Tauc, J., 1974. *Amorphous and liquid semiconductors*. New York: Plenum
- Urbach, F., 1953. The Long-Wavelength Edge of Photographic Sensitivity and of the Electronic Absorption of Solids. *Phys. Rev.*, 92: 324.
- Wahab, L.A., H.A. Zayed and A.A. Abd El-Galil, 2012. Study of structural and optical properties of Cd_{1-x}Zn_xSe thin films. *Thin Solid Films*, 520: 5195.
- Wemple, S.H., M. DiDomenico, 1971. Behavior of the Electronic Dielectric Constant in Covalent and Ionic Materials. *Phys. Rev.*, B 3: 1338.
- Zhang, X.H., Y. Guimond and Y. Bellec, 2003. Production of complex chalcogenide glass optics by molding for thermal imaging. *J. Non-Cryst. Solids*, 326-327: 519.